BONDING OF STEEL INSERTS IN Al-Si ALLOY CASTINGS

Authors: ***K. ZIMNIK[1], M. SCHÖBEL[1], H. P. DEGISCHER[1], B. REITINGER[2], U. NOSTER[3]***

Workplace: ***Inst.f.Werkstoffwissenschaft und Werkstofftechnologie, Techn.Universität Wien,***
[2] Research Center for Non Destructive TestingGmbH.,
[3]ARC Leichtmetallkompetenzzentrum Ranshofen GmbH

Abstract:

Steel inserts are embedded into Al-Si alloys by low pressure die casting and by gravity casting. SEM and LOM are used to characterize the micro-structure of the samples, particularly the interface between aluminium and steel. There is evidence of some cracks, gas entrapment, shrinkage holes and porosity detected as well by Laser Ultrasonic. Interface reactions produce Al-Fe-Si phases on cleaned steel. The Al-Si casting consists of α-dendrites with different dendrite spacings. The internal stresses in the regions of Al bulk surrounding the insert part are measured by diffraction. The compressive level of 75±25MPa in the Al Matrix originates from the quenching of the bulk. Close to the insert, the tangential stress in Al increases by about 100MPa. The bonding strength increases with the age hardening of the Mg-containing Al-Si alloy.

Keywords*:* Al-Si alloy, microstructures, solidification, shrink fit, bonding, interface

1. INTRODUCTION

Aluminium silicon alloys are well established for casting processes. Inserts of steel or cast iron provide locally increased strength and wear resistance [1, 2]. The relatively high melting temperature of iron base alloys allows to place iron parts into moulds to be surrounded by the liquid Al-melt, which solidifies embedding the insert. During solidification Al-alloys shrink by about 6vol %, but the yield strength is so low just below the solidification temperature that plastic deformation will occur around an insert. The linear coefficient of thermal expansion (CTE) of Fe is roughly half of that of Al (ΔCTE > 12ppm/K). Assuming that thermally induced elastic stresses can build up below 300°C, the misfit volume between Fe and Al amounts to about 1vol%. Assuming that the iron insert is tightly embedded into the Al alloy after casting, the shrinkage difference accumulating during cooling causes elastic and plastic straining of the Al alloy surrounding the insert. The elastic stresses building up depend on the yield strength of the alloy. An Al-Si alloy consists of α-Al-dendrites and the lamellar AlSi12 eutectic in the interdendritic regions. Mg additions allow precipitation hardening of the α-Al [3]. The room temperature yield strength of pure Al is around 50MPa, that of the AlSi12 eutectic around 150MPa. Both increase after precipitation hardening to about 150 and >200MPa respectively. Thus a linear deformation of 0.3% causes different degrees of plastic deformation within the phases of the Al alloy equilibrating the stress around the insert. The shrink fit strength depends on the micro-structure of the Al-casting. The residual stress in the Al dendrites and the interdendritic eutectic are limited by the strain hardening of the Al-matrix in the as quenched condition, which is assumed to yield less than 100MPa corresponding to about 0,1% elastic stress. After aging the yield strength increases to about 150MPa increasing the elastic stress after cooling correspondingly. Cooling from 250°C

aging temperatures produces less than 0,3% mismatch strain, at least 2/3 of which cause residual stresses.

2. DESCRIPTION OF THE METHODOLOGY

2.1 Materials

Samples of Al (99.8%), AlSi7 and AlSi7Mg0.3 with steel inserts were produced using low pressure gravity and squeeze casting processes by LKR, Austria.

Different shapes of steel inserts were used: rings, rods, cubes, and tubes. Step samples (Fig.1) contain cylindrical S355 steel inserts without surface coating (preheated to 110°C) with outer diameter of 20mm, inner diameter of 10mm. Compound samples with AlSi7Mg alloy have been manufactured by low pressure die casting with 720°C melt temperature.

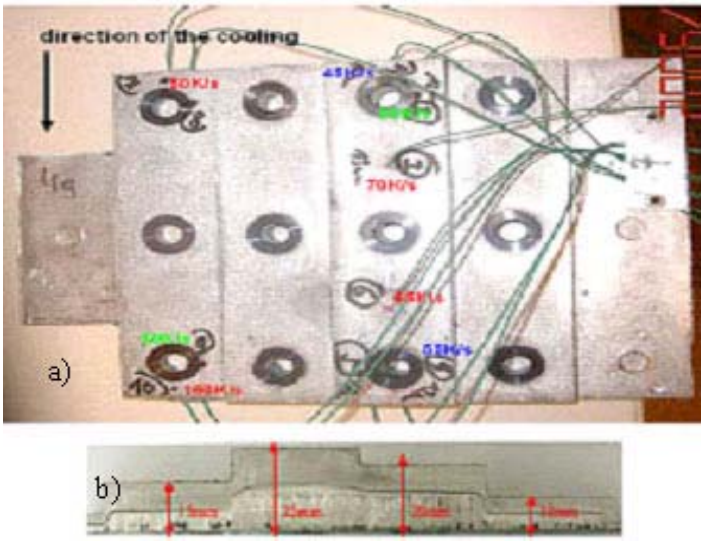

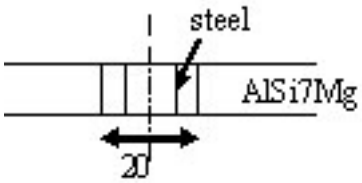

Fig.1 *a) Step sample: View of low pressure die casting with different step heights (10, 15, 20, 25 mm) with steel ring inserts and mounted thermocouples; c) sketch of the cross section shown in b)*

A demo prototype sample has been designed to demonstrate the potential of steel-aluminium composite casting [4, 5] produced by squeeze casting. It joins two inserts made from steel C45E by an AlSi7Mg cast node. It was designed to withstand axial and torsional loading by force and form lock. Fig.2 shows an exploded drawing of the demo prototype. The geometry of the steel insert is based on a tube with outer diameter of 26 mm and 3 mm wall thickness. The cross section of the steel insert smoothly varies along the axial direction from a circle to a triangular profile and widens again to a circle. The spacer ring has no mechanical function - it merely keeps the melt from flowing into the steel inserts. The demo prototype was quenched in water directly after the casting process. Some samples were aged at 160°C/2.5h 250°C/5h, and 350°C/2h.

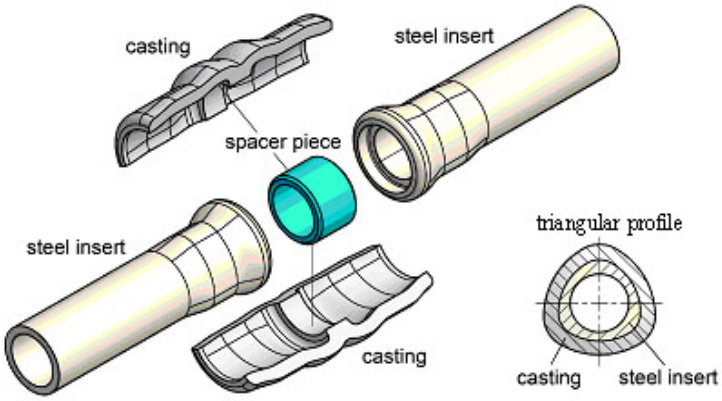

Fig.2 *Exploded drawing of the squeeze cast demo prototype with a pair of inserts of shaped steel tubes [5] and the cross section of the triangular segment*

The gravity casting consists of suspended rod steel inserts, which is surrounded by AlSi7 cast at different melt temperatures (700°C and 750°C). Different surface treatments (oxidized and etched) were carried out to study the effect of interface reactions [6, 7] by SEM.

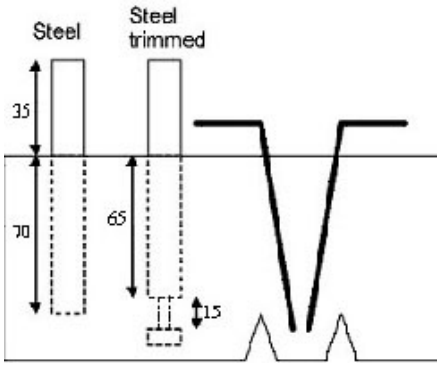

Fig.3 *View of the gravity castings with inserted steel rods*

3.2 Characterisation methods

Light optical microscopy was used to characterize the micro-structure of the casting and of the interface between aluminium and steel insert. The aim of the SEM analysis was to look for the intermetallic reaction phases, cracks and the bonding between Al and steel insert. The internal stresses of the aluminium around the steel insert were measured by X-ray diffraction, where the $\sin^2\Psi$ method was used. The neutron diffraction measurements were performed at Helmholtz Zentrum Berlin [8]. The temperature dependence of the yield strength of the Al-alloy was determined by hot compression tests using a Gleeble Machine 1500. Thermal cycling experiments and push out tests were performed using slices taken from a sample with a rod insert. Pull and push out tests were performed with as cast and heat treated demo-prototype samples. The force of the bonding between steel and Al was measured by a Zwick Z050. Laser ultrasound (LUS) is a non-destructive method [9, 10] to detect very high frequency ultrasound waves generated by focusing a pulsed high energy laser with pulse times of picoseconds to nanoseconds on to the surface of a sample. Bulk waves [11] were generated by focussing picoseconds laser pulses with energies of 5mJ to a small spot on the inner side of the steel tube. On the opposite side (on the aluminium surface) the arriving bulk waves are detected by the photorefractive detector. The interface of the sample is scanned by revolution of the sample and by subsequently stepping along the X-axis.

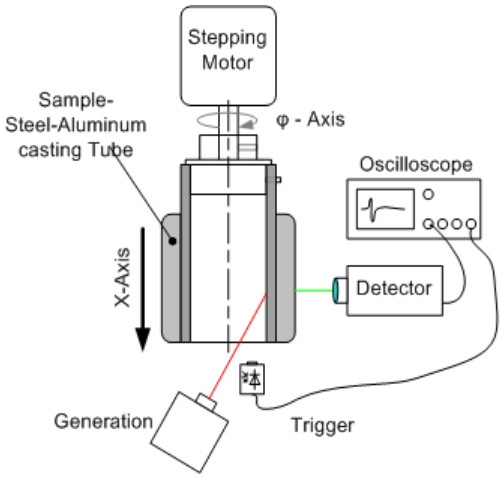

Fig.4 *Measurement setup for non destructive Laser generated ultra sound wave detection; Laser beam scanned the inner cylinder while the detectors canned the outside*

4. RESULTS

4.1 Light Optical Microscopy

Looking at the plane through the middle of the thickness of the step samples, we can see gaps between the insert and the casting in some places, but these do not open continuously (Fig.5a). The shape of the gaps indicates that they were formed during solidification owing to gas entrapment. We can observe eutectic zones at the bonded interface in Fig.5b. There, the secondary dendrite arms measure of about 15µm. Fig.5c shows the borders of the Al casting towards the gap. There, the direction of the solidification i.e. orientation of the dendrites, can be concluded to be from the bulk to the gap. The changes in solidification rate are indicated by the size of the dendrite arms.

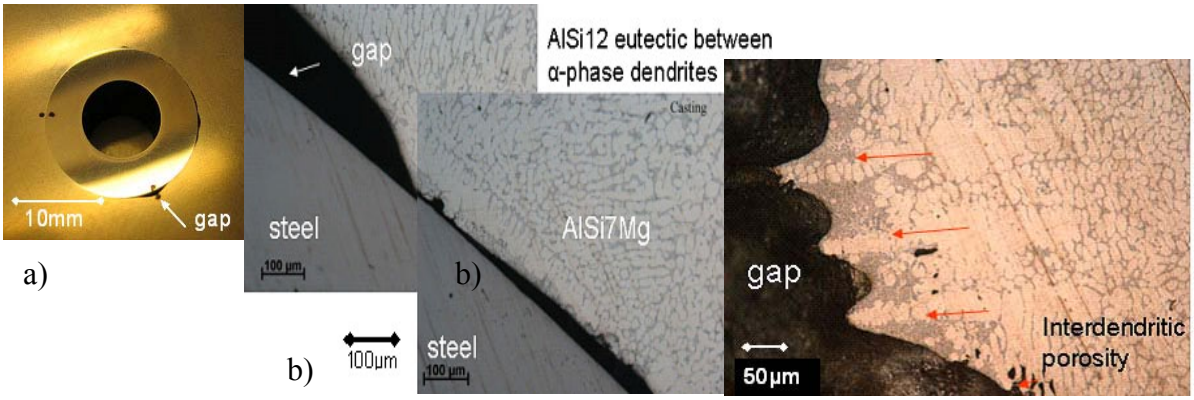

Fig. 5 *LOM micrographs at the inert with local gaps: a) Image of the central cut through a cylinder insert in the step sample, c) dendrites of the Al-Si casting surrounding by local gaps*

4.2 Scanning Electron Microscopy

Interface reactions took place at the faces of contact between steel rod and Al-Si melt. 10µm to 50µm islands of intermetallic phases are formed when the mould was heated [Fig.6). The intermetallic phase [6] grows into the steel in a columnar front. Cracks in those reaction layers were in all of the investigated samples. Some Fe got dissolved in the liquid Al, which segregated during solidification forming Al-Fe-Si -inclusions on the Al-side [3]. The thermally induced interface shear stresses are relieved by cracks.

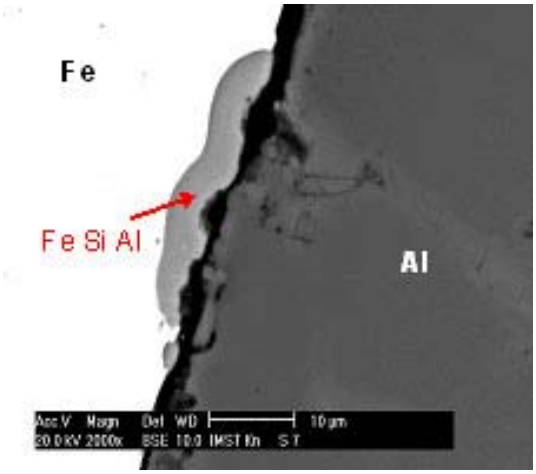

Fig.6 *Micrographs showing intermetallic islands on the cross section of the rod steel insert in AlSiMg*

4.3 Diffraction

The internal stresses of the aluminium around the steel insert after the casting process were measured by X-ray diffraction. The reflections were evaluated by $\sin^2\Psi$ method [11]. Fig.7 shows the stress analysis of the investigated Al casting after heating to 350°C and quenching. The radial and tangential stress values measured in the Al phase long radial line from the steel interface. Only the region close to the interface to the steel insert shows tangential tensile stresses in Fig.7, more than 100MPa above the more or less isotropic compressive stress level further away.

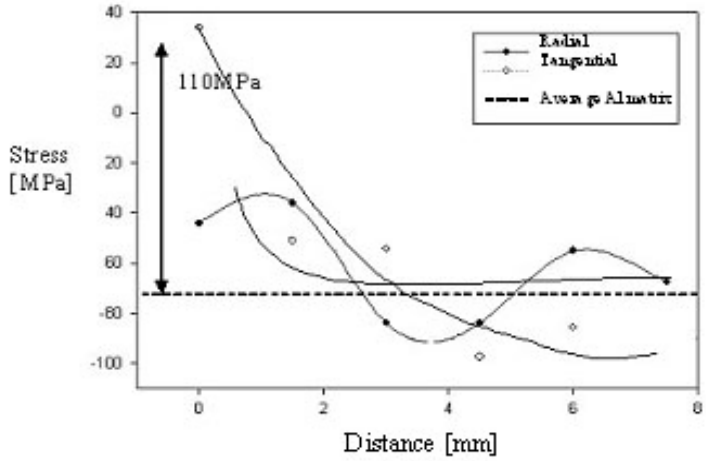

Fig.7 *Stress analysis by X-ray diffraction of the Al in the cast alloy quenched from 350°C along a radial line from the steel interface compared with stress values measured in AlSi7 without steel insert*

Stress changes in Al and Si in an AlSi7 alloy without insert were measured after quenching from different temperatures by neutron diffraction, the results of which are shown in Fig.8.

Negligibly stress as were measured in a cast AlSi7 sample in α-Al and in Si in an as received T1 condition. After reheating and quenching in water residual stresses increase with increasing quenching temperature reaching above 90MPa compression stress in Al and more than 100MPa tensile stress in Si.

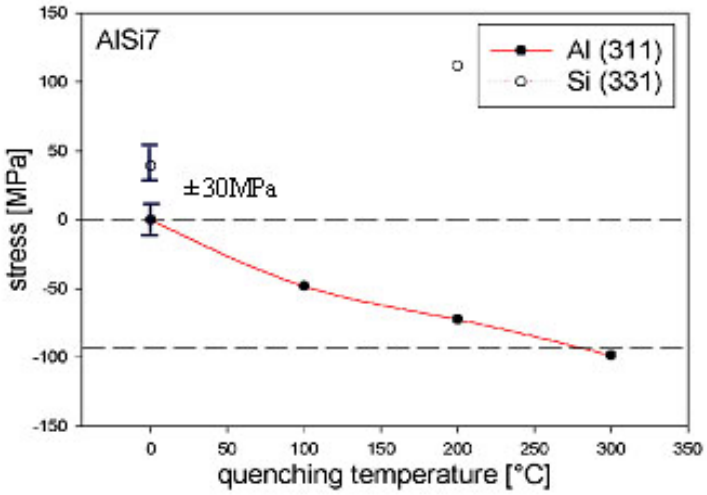

Fig. 8 *Stress change in Al and Si in AlSi7 alloy without insert after quenching from different temperatures (neutron diffraction results)*

4.4 Laser ultrasound tests (LUS)

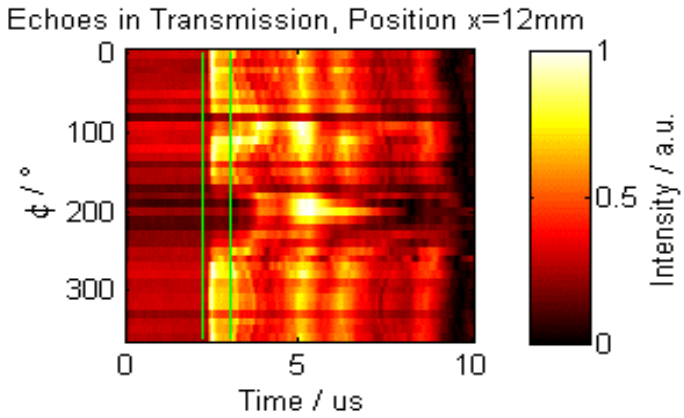

Fig. 9 *Ultrasonic raw data of one 360° scan. The green lines show the limits for subsequent longitudinal peak identification*

Figure 9 shows the LUS measurement result for an entire 360° rotation at a certain X-value. The first arriving longitudinal bulk wave can be identified at approximately 2.2µs. A defect can be identified by very low signal amplitude between 170° and 250° rotation. This defect can be interpreted as a debonding between steel and aluminum. Fig.10a shows the maximum amplitudes between 2µs and 3µs (the green lines in figure 9) along the X-axis and φ-rotation. A defect shows up with very small amplitudes in the region of 10-15mm and at angles between 170° and 250°. Figure 10b shows the positions of the maxima, a second defect can be seen at rotation angles between 60° and 100°.

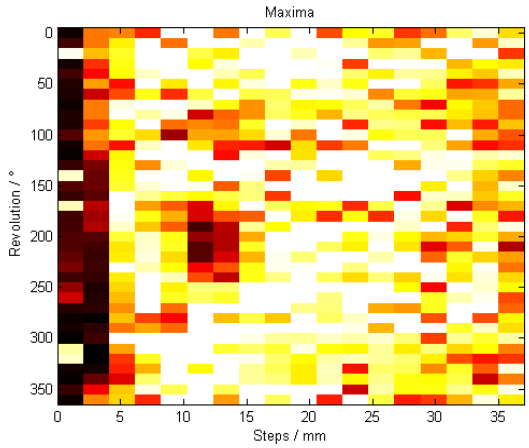

Fig. 10 a) *Scan along the surface of the sample. Amplitudes of signals between 2µs and 3µs are shown. Darker colours indicate weaker amplitudes of the arriving longitudinal wave*

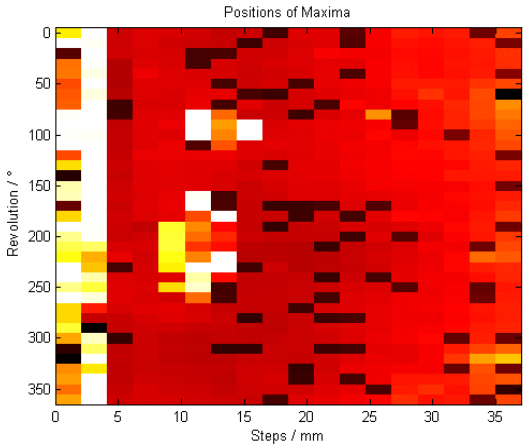

Fig. 10 b) *Scan along the surface with the positions x of the maxima shown. Brighter colours indicate a later arrival of the longitudinal waves*

4.5 Mechanical tests

Push out tests were performed with as cast and heat treated demo-prototype samples. The force of the bonding between steel and Al was measured by a Zwick Z050. The results of the push out tests of the demo prototype sample are shown in Fig.11. The bonding between steel and Al is stronger after age than in as cast samples. Highest strength is observed for the peak aged sample #22.

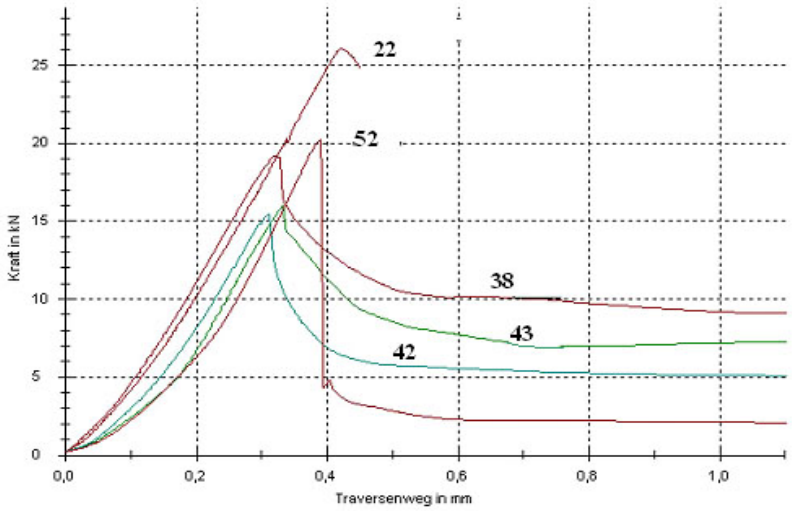

Sample	Condition
22	165°C / 2,5h
52	250°C / 5h
38	250°C / 5h
43	As cast
42	As cast

Fig.11 *Push out test of the steel tubes from the as cast and heat treated demo prototype: force versus displacement curves*

5. DISCUSSIONS OF RESULTS

The Al-Si-castings consist of α-dendrites and eutectic Al-Si12. The different secondary dendrite arm spacings (SDA) reflect the local cooling rate in the mould. Close to the mould, the SDA are much smaller, which means that solidification started from the mould. Gaps occur around the insert in most of the samples, caused by gas entrapment, when the solidification front arrived.

There is evidence of inter dendritic shrinkage porosity at the interface. In some cases, a second solidification front starts from the cold insert. If solidification starts at the interface (in a hot mould) embedding fails due to heat transfer to the insert, remelting and a second solidification path from the mould causing significant porosity. Shrinkage strains develop not only around the steel insert, but as well in longitudinal direction causing glide and occasionally cracking. Interface reactions were observed extensively on cleaned steel inserts with pure Al castings, but only locally for Al-Si castings. Interface reaction zones do not improve the bonding strength due to cracks. Age hardening of the AlSi7Mg alloy improves the bonding strength due the increase in elastic shrink fitting strains. The tangential stresses around the insert could not be measured reliably (>30MPa tensile). There is a compressive stress background (-90MPa) within the α-Al phase due to the expansion mismatch between Al and Si (ΔCTE > 20ppm/K). On top of that circumferential tensile stresses are superimposed at the border to the insert.

6. CONCLUSIONS

- Embedding a steel insert into an Al-casting requires, that solidification starts at the interface. The heat balance shall keep the insert well below the solidus temperature of the alloy. No twofold solidification process (second from the mould wall) should operate.

- The interface reactions of the investigated cases showed no effect to the bonding strength tested in push out experiments. Crack initiation in the Al-Fe interface reaction zone occurs during cooling from the melt.

- Bonding strength is increased by increasing the yield strength of the embedding Al alloy by age hardening.

- The residual stress in Al-Si alloys cause significant compressive stress in α-Al during cooling. Circumferential tensile stresses are superimposed close (<2mm) to the interface with the steel insert.

- LUS can be used for tubular inserts for non destructive testing of the interface quality.

Acknowledgements

The authors would like to thank the ARC Leichtmetallkompetenzzentrum Ranshofen GmbH (LKR)/Austria for casting the samples. The authors are grateful to Mr. W.Fragner, Mr. Z.Khalil, Mr. R.Bitsche, Mrs. H.Knoblich and Mrs. A.Danninger for they collaboration in the preparation of this paper. The ALWS project was funded mainly by the Austrian Nationalstiftung für Forschung, Technologie und Entwicklung.

References

[1] DAVIS, J., R. *ASM Specialty Handbook*. Aluminum and aluminium alloys, 1993.

[2] NISSLE, S., DASSLER, S., NOSTER, U., MUNDL, A. *Neue Auslegungsmöglichkeiten für Gussteile durch Funktionsintegration oder lokale Verstärkung*. Tagungsbd. d. 5. Ranshofener Leichtmetalltage, LKR-Verlag, Ranshofen 2008, 35-44

[3] POLMEAR, I., J. *Light Alloys, Metallurgy of the light metals*. Third edition, 1995.

[4] BITSCHE, R., D., NOSTER, U., PETERLECHNER, C., RAMMERSTORFER, F.,G. *Simulation von kraft- und formschlüssigen Hybridguss-Verbindungen als Designgrundlage*. Tagungsbd. d 4. Ranshofener Leichtmetalltage, LKR-Verlag, Ranshofen, 2006, 275-286

[5] BITSCHE, R., D. *Dissertation.* Technische Universität Wien, 2009

[6] KUBASCHEWSKI, O. *Iron-Binary Phase Diagrams*. Springer-Verlag Berlin, 1982.

[7] EGGELER, G., AUER, W., KAESCHE, H. On the influence of silicon on the growth of the alloy layer during hot dip aluminizing. In *Journal of Materials.* 21, 1986.

[8] www.hmi.de

[9] SCRUBY, C., B., AND DRAIN, L., E. *Laser ultrasonics: Techniques and applications*. Adam Hilger, 1990.

[10] MONCHALIN J., P. *Optical Detection of Ultrasound, IEEE Transactions on Ultrasonic, Ferroelectrics, and Frequency Control*. 1986, Vol.UFFC-33, No.5, 485-499

[11] WANG, X., XU, X. Thermoel. wave induced by pulsed laser heating. In *Appl.Phys.* A 73, 2001, 107–114

[12] REIMERS, W., PYZALLA, A.,R., SCHREYER, A., Clemens, H. *Neutrons and Synchrotron Radiation in Engineering Materials Science*. WILEY-VCH Verlag GmbH & Co KGaA